EUROPEAN ORGANISATION FOR NUCLEAR RESEARCH

CERN-PPE/92-213
11 December, 1992

A Measurement of $K^*(892)^{\pm}$ Production in Hadronic Z^0 Decays

The OPAL Collaboration

Abstract

Measurements are presented of the inclusive cross section for $K^*(892)^{\pm}$ production in hadronic decays of the Z^0, using a sample of about half a million events recorded with the OPAL experiment at LEP. Charged K^* mesons are reconstructed in the decay channel $K^0_S\pi^{\pm}$. A mean rate of $0.72 \pm 0.02 \pm 0.08$ $K^{*\pm}$ mesons per hadronic event is found. Comparison of the results with predictions of the JETSET and HERWIG models shows that JETSET overestimates the $K^{*\pm}$ production cross section while HERWIG is consistent with the data.

Submitted to Physics Letters B

The OPAL Collaboration

P.D. Acton[25], G. Alexander[23], J. Allison[16], P.P. Allport[5], K.J. Anderson[9], S. Arcelli[2], A. Astbury[28], D. Axen[29], G. Azuelos[18,a], G.A. Bahan[16], J.T.M. Baines[16], A.H. Ball[17], J. Banks[16], R.J. Barlow[16], S. Barnett[16], J.R. Batley[5], G. Beaudoin[18], A. Beck[23], J. Becker[10], T. Behnke[27], K.W. Bell[20], G. Bella[23], P. Bentkowski[18], P. Berlich[10], S. Bethke[11], O. Biebel[3], U. Binder[10], I.J. Bloodworth[1], P. Bock[11], B. Boden[3], H.M. Bosch[11], S. Bougerolle[29], H. Breuker[8], P. Bright-Thomas[25], R.M. Brown[20], A. Buijs[8], H.J. Burckhart[8], C. Burgard[27], P. Capiluppi[2], R.K. Carnegie[6], A.A. Carter[13], J.R. Carter[5], C.Y. Chang[17], D.G. Charlton[8], P.E.L. Clarke[25], I. Cohen[23], J.C. Clayton[1], W.J. Collins[5], J.E. Conboy[15], M. Cooper[22], M. Coupland[14], M. Cuffiani[2], S. Dado[22], G.M. Dallavalle[2], S. De Jong[8], L.A. del Pozo[5], H. Deng[17], A. Dieckmann[11], M. Dittmar[4], M.S. Dixit[7], E. do Couto e Silva[12], J.E. Duboscq[8], E. Duchovni[26], G. Duckeck[11], I.P. Duerdoth[16], D.J.P. Dumas[6], P.A. Elcombe[5], P.G. Estabrooks[6], E. Etzion[23], H.G. Evans[9], F. Fabbri[2], M. Fincke-Keeler[28], H.M. Fischer[3], D.G. Fong[17], M. Foucher[17], A. Gaidot[21], O. Ganel[26], J.W. Gary[4], J. Gascon[18], R.F. McGowan[16], N.I. Geddes[20], C. Geich-Gimbel[3], S.W. Gensler[9], F.X. Gentit[21], G. Giacomelli[2], V. Gibson[5], W.R. Gibson[13], J.D. Gillies[20], J. Goldberg[22], M.J. Goodrick[5], W. Gorn[4], C. Grandi[2], F.C. Grant[5], J. Hagemann[27], G.G. Hanson[12], M. Hansroul[8], C.K. Hargrove[7], P.F. Harrison[13], J. Hart[8], P.M. Hattersley[1], M. Hauschild[8], C.M. Hawkes[8], E. Heflin[4], R.J. Hemingway[6], R.D. Heuer[8], J.C. Hill[5], S.J. Hillier[1], T. Hilse[10], D.A. Hinshaw[18], J.D. Hobbs[8], P.R. Hobson[25], D. Hochman[26], R.J. Homer[1], A.K. Honma[28,a], R.E. Hughes-Jones[16], R. Humbert[10], P. Igo-Kemenes[11], H. Ihssen[11], D.C. Imrie[25], A.C. Janissen[6], A. Jawahery[17], P.W. Jeffreys[20], H. Jeremie[18], M. Jimack[2], M. Jobes[1], R.W.L. Jones[13], P. Jovanovic[1], C. Jui[4], D. Karlen[6], K. Kawagoe[24], T. Kawamoto[24], R.K. Keeler[28], R.G. Kellogg[17], B.W. Kennedy[15], S. Kluth[5], T. Kobayashi[24], D.S. Koetke[8], T.P. Kokott[3], S. Komamiya[24], L. Köpke[8], J.F. Kral[8], R. Kowalewski[6], J. von Krogh[11], J. Kroll[9], M. Kuwano[24], P. Kyberd[13], G.D. Lafferty[16], R. Lahmann[17], F. Lamarche[18], J.G. Layter[4], P. Leblanc[18], A.M. Lee[17], M.H. Lehto[15], D. Lellouch[26], C. Leroy[18], J. Letts[4], S. Levegrün[3], L. Levinson[26], S.L. Lloyd[13], F.K. Loebinger[16], J.M. Lorah[17], B. Lorazo[18], M.J. Losty[7], X.C. Lou[12], J. Ludwig[10], M. Mannelli[8], S. Marcellini[2], G. Maringer[3], C. Markus[3], A.J. Martin[13], J.P. Martin[18], T. Mashimo[24], P. Mättig[3], U. Maur[3], J. McKenna[28], T.J. McMahon[1], J.R. McNutt[25], F. Meijers[8], D. Menszner[11], F.S. Merritt[9], H. Mes[7], A. Michelini[8], R.P. Middleton[20], G. Mikenberg[26], J. Mildenberger[6], D.J. Miller[15], R. Mir[12], W. Mohr[10], C. Moisan[18], A. Montanari[2], T. Mori[24], M. Morii[24], T. Mouthuy[12,b], B. Nellen[3], H.H. Nguyen[9], M. Nozaki[24], S.W. O'Neale[1], F.G. Oakham[7], F. Odorici[2], H.O. Ogren[12], C.J. Oram[28,a], M.J. Oreglia[9], S. Orito[24], J.P. Pansart[21], B. Panzer-Steindel[8], P. Paschievici[26], G.N. Patrick[20], N. Paz-Jaoshvili[23], P. Pfister[10], J.E. Pilcher[9], J. Pinfold[31], D. Pitman[28], D.E. Plane[8], P. Poffenberger[28], B. Poli[2], A. Pouladdej[6], E. Prebys[8], T.W. Pritchard[13], H. Przysiezniak[18], G. Quast[27], M.W. Redmond[9], D.L. Rees[8], G.E. Richards[16], D. Robinson[8], A. Rollnik[3], J.M. Roney[28,c], E. Ros[8], S. Rossberg[10], A.M. Rossi[2], M. Rosvick[28], P. Routenburg[6], K. Runge[10], O. Runolfsson[8], D.R. Rust[12], M. Sasaki[24], C. Sbarra[8], A.D. Schaile[10], O. Schaile[10], W. Schappert[6], P. Scharff-Hansen[8], P. Schenk[28], B. Schmitt[3], H. von der Schmitt[11], S. Schreiber[3], C. Schwick[27], J. Schwiening[3], W.G. Scott[20], M. Settles[12], T.G. Shears[5], B.C. Shen[4], C.H. Shepherd-Themistocleous[7], P. Sherwood[15], R. Shypit[29], A. Simon[3], P. Singh[13], G.P. Siroli[2], A. Skuja[17], A.M. Smith[8], T.J. Smith[8], G.A. Snow[17], R. Sobie[28,c], R.W. Springer[17], M. Sproston[20], K. Stephens[16], J. Steuerer[28], R. Ströhmer[11], D. Strom[30], T. Takeshita[24,d], P. Taras[18], S. Tarem[26], M. Tecchio[9], P. Teixeira-Dias[11], N. Tesch[3], N.J. Thackray[1], M.A. Thomson[15], E. Torrente-Lujan[22],

G. Transtromer[25], N.J. Tresilian[16], T. Tsukamoto[24], M.F. Turner[8], G. Tysarczyk-Niemeyer[11], D. Van den plas[18], R. Van Kooten[8], G.J. VanDalen[4], G. Vasseur[21], C.J. Virtue[7], A. Wagner[27], D.L. Wagner[9], C. Wahl[10], J.P. Walker[1], C.P. Ward[5], D.R. Ward[5], P.M. Watkins[1], A.T. Watson[1], N.K. Watson[8], M. Weber[11], P. Weber[6], S. Weisz[8], P.S. Wells[8], N. Wermes[3], M.A. Whalley[1], G.W. Wilson[4], J.A. Wilson[1], V-H. Winterer[10], T. Wlodek[26], S. Wotton[11], T.R. Wyatt[16], R. Yaari[26], A. Yeaman[13], G. Yekutieli[26], M. Yurko[18], W. Zeuner[8], G.T. Zorn[17].

[1]School of Physics and Space Research, University of Birmingham, Birmingham, B15 2TT, UK
[2]Dipartimento di Fisica dell' Università di Bologna and INFN, Bologna, 40126, Italy
[3]Physikalisches Institut, Universität Bonn, D-5300 Bonn 1, FRG
[4]Department of Physics, University of California, Riverside, CA 92521 USA
[5]Cavendish Laboratory, Cambridge, CB3 0HE, UK
[6]Carleton University, Dept of Physics, Colonel By Drive, Ottawa, Ontario K1S 5B6, Canada
[7]Centre for Research in Particle Physics, Carleton University, Ottawa, Ontario K1S 5B6, Canada
[8]CERN, European Organisation for Particle Physics, 1211 Geneva 23, Switzerland
[9]Enrico Fermi Institute and Department of Physics, University of Chicago, Chicago Illinois 60637, USA
[10]Fakultät für Physik, Albert Ludwigs Universität, D-7800 Freiburg, FRG
[11]Physikalisches Institut, Universität Heidelberg, Heidelberg, FRG
[12]Indiana University, Dept of Physics, Swain Hall West 117, Bloomington, Indiana 47405, USA
[13]Queen Mary and Westfield College, University of London, London, E1 4NS, UK
[14]Birkbeck College, London, WC1E 7HV, UK
[15]University College London, London, WC1E 6BT, UK
[16]Department of Physics, Schuster Laboratory, The University, Manchester, M13 9PL, UK
[17]Department of Physics, University of Maryland, College Park, Maryland 20742, USA
[18]Laboratoire de Physique Nucléaire, Université de Montréal, Montréal, Quebec, H3C 3J7, Canada
[20]Rutherford Appleton Laboratory, Chilton, Didcot, Oxfordshire, OX11 0QX, UK
[21]DAPNIA/SPP, Saclay, F-91191 Gif-sur-Yvette, France
[22]Department of Physics, Technion-Israel Institute of Technology, Haifa 32000, Israel
[23]Department of Physics and Astronomy, Tel Aviv University, Tel Aviv 69978, Israel
[24]International Centre for Elementary Particle Physics and Dept of Physics, University of Tokyo, Tokyo 113, and Kobe University, Kobe 657, Japan
[25]Brunel University, Uxbridge, Middlesex, UB8 3PH UK
[26]Nuclear Physics Department, Weizmann Institute of Science, Rehovot, 76100, Israel
[27]Universität Hamburg/DESY, II Inst für Experimental Physik, 2000 Hamburg 52, Germany
[28]University of Victoria, Dept of Physics, P O Box 3055, Victoria BC V8W 3P6, Canada
[29]University of British Columbia, Dept of Physics, 6224 Agriculture Road, Vancouver BC V6T 1Z1, Canada
[30]University of Oregon, Dept of Physics, Eugene, Oregon 97403, USA
[31]University of Alberta, Dept of Physics, Edmonton AB T6G 2J1, Canada

[a]Also at TRIUMF, Vancouver, Canada V6T 2A3
[b]Now at Centre de Physique des Particules de Marseille, Faculté des Sciences de Luminy, Marseille

[c]And IPP, University of Victoria, Dept of Physics, P O Box 3055, Victoria BC V8W 3P6, Canada
[d]Also at Shinshu University, Matsumoto 390, Japan

Introduction

Inclusive spectra of particles produced in electron positron collisions have been studied extensively in order to shed light on the process of hadronization, whereby coloured partons are confined inside colourless hadrons. Since perturbation theory is not applicable to this stage of an e^+e^- event, one has to rely on phenomenological models.

Amongst the most successful ones are the string [1] and the cluster fragmentation [2] models, both of which were developed at PETRA and PEP energies where they were tested extensively. Recently, measurements of inclusive distributions of π^0 [3], K^0_S [4], $K^*(892)^{\pm}$, Λ, Ξ^- [5], η,η' [6], $K^*(892)^0$, ϕ [7], ρ^0, $f_0(975)$, $f_2(1270)$ [8], and Λ, Ξ^-, $\Sigma^{\pm}(1385)$, $\Xi^0(1530)$, and Ω^- [9] (and the corresponding antiparticles) have become available at centre of mass energies around the Z^0 pole.

In this paper, we present a study of $K^*(892)^{\pm}$ production in e^+e^- collisions at $\sqrt{s} \simeq M_{Z^0}$ using approximately 500,000 events recorded with the OPAL detector in 1990 and 1991. $K^{*\pm}$ mesons were reconstructed via their decay $K^{*\pm} \rightarrow K^0_S\pi^{\pm}$, with the K^0_S subsequently decaying into $\pi^+\pi^-$. A clean K^0_S signal was obtained by reconstruction of K^0_S decaying at a secondary vertex well separated from the interaction point. The $K^{*\pm}$ signal observed in the invariant mass distribution of $K^0_S\pi^{\pm}$ combinations, however, is located on top of a large combinatorial background due to the large charged multiplicity.

The OPAL Detector and Hadronic Event Selection

The OPAL detector, a multi–purpose detector designed to measure the decay products of the Z^0 boson, has been described in detail elsewhere [10]. Here, we briefly describe the components most relevant for the present analysis, namely, the central tracking chambers.

The main tracking device is a large cylindrical drift chamber of the jet type with 4 m length and a diameter of 3.7 m. It is subdivided into 24 identical sectors, each of which is equipped with 159 sense wires, providing a large number of measured space points per track. The momentum resolution was measured to be $\sigma_{p_t}/p_t = \sqrt{0.02^2 + (0.0018 \cdot p_t)^2}$ [11], where p_t in GeV/c is the momentum component transverse to the beam axis. The z coordinate along the beam direction is measured with the charge division method. The vertex detector, a small, high–resolution drift chamber of 1 m length and 470 mm diameter, is located close to the interaction point inside the jet chamber. It consists of 36 axial sectors in the inner region, each with 12 sense wires, and 35 stereo sectors in the outer region, each with 6 sense wires. The jet chamber is surrounded by the z–chambers, planar drift chambers with wires perpendicular to those of the jet chamber, providing accurate measurements of the z–coordinate[1]. They are composed of 24 drift chambers, 4 m long and 50 cm wide, each subdivided into 8 cells with 6 sense wires. The polar angular range from 44° to 136° is covered. The tracking chambers are contained in a solenoid providing an axial magnetic field of 0.435 T.

The selection of hadronic events is based on the information of the jet chamber and the electromagnetic calorimeter. A good track is defined to have at least 20 measured points in the jet chamber, and to originate from a cylinder of 800 mm length and 20 mm diameter centered around the interaction point. A cluster is defined as an energy deposition in the electromagnetic calorimeter exceeding 100 MeV in the region $|\cos\theta| < 0.82$ or 200 MeV in the

[1] A right-handed coordinate system is adopted by OPAL, where the x axis points to the centre of the LEP ring, and positive z is along the electron beam direction. The angles θ and ϕ are the polar and azimuthal angles, respectively.

region $|\cos\theta| > 0.82$. Events were required to possess at least 5 good tracks and 7 clusters. Furthermore, the total energy deposited in the electromagnetic calorimeter had to exceed 10 % of the centre of mass energy, and the energy imbalance along the beam direction, defined by $|\sum_i E_i \cdot \cos\theta_i| / \sum_i E_i$, where the sum runs over all clusters, was required to be smaller than 0.65. Further details of the electromagnetic calorimeter can be found in [10]. With this hadronic event selection, in combination with the additional requirement that the tracking chambers had to be fully operational, a total of 471 952 hadronic events was selected.

Selection of charged K^* mesons

The first step in the $\mathrm{K}^{*\pm}$ selection process was the identification of K^0_S mesons decaying into $\pi^+\pi^-$. The algorithm is identical to the one described in [4]. Briefly, oppositely charged tracks were combined to make up K^0_S candidates. The tracks were required to have a minimum transverse momentum with respect to the beam direction of 150 MeV/c, at least 80 jet chamber hits and 4 z-chamber hits. The last condition limits the polar angle region covered to $|\cos\theta| < 0.72$. Furthermore, the radial distance of the track to the beam axis at the point of closest approach was required to exceed 3 mm to reduce the large combinatorial background.

Intersection points of track pairs in the radial plane were considered to be candidate secondary vertices. Additional cuts were imposed on these pairs: the radial distance from the intersection point to the primary vertex had to be larger than 1 cm and the reconstructed momentum vector of the K^0_S candidate in the plane perpendicular to the beam had to point to the beam axis to within 2°. Finally, all track pairs which had passed the cuts were refitted with the constraint that they originate from a common 3-dimensional vertex. Pairs with an invariant mass of less than 100 MeV/c^2 (assuming both tracks to be electrons) were considered to be photon conversions and were rejected. About 50000 K^0_S candidates were selected.

For the further analysis, only K^0_S candidates with a reconstructed mass in a window of ± 30 MeV/c^2 around the nominal mass of 497.7 MeV/c^2 were retained. To construct a $\mathrm{K}^{*\pm}$ candidate, these K^0_S candidates were combined with a third charged track which was assumed to be a pion. This track had to meet the following conditions. The minimum transverse momentum and the minimum number of jet chamber hits were the same as for the K^0_S selection. The polar angle of the track had to satisfy $|\cos\theta| < 0.7$, and the distance of the track to the interaction point in the plane perpendicular to the beam had to be smaller than 2.5 mm. In order to improve the mass resolution, the track was constrained to the event vertex in the z direction.

Additional cuts were imposed on these $\mathrm{K}^0_\mathrm{S}\pi^\pm$ combinations to improve the signal to background ratio: the cosine of the angle between the K^0_S candidate and the third track had to be larger than 0. The pion candidate was boosted into the $\mathrm{K}^0_\mathrm{S}\pi^\pm$ rest frame and the angle θ^* of the boosted pion momentum with respect to the K^* flight direction had to fulfill the condition $\cos\theta^* > -0.7$. This cut further reduces the combinatorial background which is particularly large in the excluded region of $\cos\theta^*$.

Finally, the nominal value of the K^0 mass was assigned to the K^0_S candidate, and the invariant masses of the $\mathrm{K}^0_\mathrm{S}\pi^\pm$ combinations were calculated. The resulting distribution is shown in figure 1. The signal due to the $\mathrm{K}^{*\pm}$ can be clearly observed; a fit with contributions from a Breit–Wigner shape and the smooth background described below yields a $\mathrm{K}^{*\pm}$ mass of 889 ± 2 MeV/c^2 consistent with the world average of 891.8 MeV/c^2 [12]. For the width, Γ, we measure 60 ± 5 MeV/c^2 in good agreement with the result of 55 ± 2 MeV/c^2 for a Monte Carlo generated event sample with full detector simulation [13]. If folded with the OPAL detector mass resolution,

both values are consistent with the intrinsic width of the $K^{*\pm}$ of 49.8 MeV/c^2 [12]. About 7200 $K^{*\pm}$ are contained in the peak.

To determine the cross section for $K^{*\pm}$ production, the separation of the remaining large background from the signal is crucial. For this purpose, fits to the mass spectra were performed in intervals of the $K^{*\pm}$ momentum. For the signal, a Breit–Wigner shape was used with the mass fixed to the nominal value. An effective width per momentum interval with contributions from the $K^{*\pm}$ intrinsic width and the momentum dependent detector mass resolution was calculated using the OPAL detector simulation [13]. The widths were fixed to these values. To describe the background, two different shapes have been employed, namely

$$b_1(m) = P_1 \cdot (m - m_0)^{P_2} \cdot \exp(-P_3 m - P_4 m^2), \quad (1)$$

$$b_2(m) = P_1 \cdot \left(1 - \exp\left(\frac{-(m - m_0)}{P_2}\right)\right) \cdot \exp(-P_3 m - P_4 m^2). \quad (2)$$

The P_i are free parameters, with $m_0 = m_{K^0_S} + m_\pi$ being the kinematical mass threshold. In each momentum interval, the background shape leading to the better χ^2 has been taken while the other was used in assessing the systematic uncertainties, as described below. The fits are shown in figure 2.

The $K^{*\pm}$ cross section

To account for the loss of $K^{*\pm}$ due to geometrical acceptance and selection cuts, we proceeded in two steps. First, the loss due to the requirement that both tracks from the K^0_S decay have associated z–chamber hits was calculated from data, since the z–chamber efficiency is slightly overestimated by the detector simulation. To that end, the z–chamber efficiency was measured using charged tracks [4]. The mass spectra shown in figure 2 have already been corrected for these z-chamber inefficiencies. Then, the detection efficiency (not including the z–chamber efficiency) was calculated using a sample of events generated with the JETSET program and passed through a detailed simulation of the OPAL detector [13]. These events were subjected to the same analysis chain as the real data.

Finally, the branching ratios for $K^{*\pm} \to K^0\pi^\pm$ and $K^0_S \to \pi^+\pi^-$ were corrected for and a factor of 2 was applied to account for the fact that half of the kaons produced appear as K^0_L and are not found in the detector.

As sources of possible systematic errors, we identified contributions from the uncertainty arising from the background separation and the signal shape, from uncertainty in the mass resolution and from the uncertainty of the detection efficiency. The error from the background separation was estimated by comparing the results from the different background parametrizations (equations 1, 2) and from a variation of the mass range included in the fit. Furthermore, the same background separation procedure was applied to simulated events, where the precise fractions of signal and background are known, permitting an additional estimate of the accuracy of the method. An uncertainty of 20 % per momentum interval was found from these studies. Since the background shape is different in each momentum interval, the errors are largely uncorrelated and thus contribute 10 % to the integrated rate. The contribution from the signal shape was investigated by fitting a relativistic Breit–Wigner function for the signal instead of the standard Breit–Wigner shape; the results were found to be identical to within 2 %. Furthermore, the fit was repeated with a $K^{*\pm}$ mass fixed to values shifted by ± 2 MeV from the nominal value; differences were below 1 %. Thus, uncertainties from the signal shape

and position are negligible compared to the errors from the background separation. The mass resolution in the Monte Carlo simulation was slightly better than in the real data. However, the K^* intrinsic width dominates the observed width, and only relatively small contributions to the systematic errors arose from this source. To assess the uncertainty from the detection efficiency, a detailed comparison of distributions from real and simulated events has been performed. In addition, the selection cuts were varied and the analysis was repeated. By these means, an uncertainty in the detection efficiency of 4 % was obtained.

The differential cross section $1/(\beta\sigma_{had})(d\sigma/dx_E)$ for $K^{*\pm}$ production as a function of the scaled $K^{*\pm}$ energy, $x_E = 2E_{K^*}/\sqrt{s}$, is shown in figure 3 and table 1 (here β is the particle velocity, p/E). The $K^{*\pm}$ multiplicity per hadronic event, obtained by integration of the differential cross section, is $0.72 \pm 0.02 \pm 0.08$. The first error quoted is statistical and the second stems from systematic uncertainties.

Our measured multiplicity is considerably lower than the result of [5], where a rate of $1.33 \pm 0.11 \pm 0.24$ is given. The $K^{*\pm}$ multiplicity is expected to be similar to the rate of neutral K^* mesons, which has been measured to be $0.76 \pm 0.07 \pm 0.06$ [7], in good agreement with our $K^{*\pm}$ rate.

Comparison with model predictions

Besides our measured values, figure 3 also shows the predictions of the JETSET [14] (Version 7.2) and HERWIG [15] (Version 5.0) models. The fragmentation parameters of these programs were tuned to describe the global event shapes as measured by OPAL[2] [16].

The predicted cross sections are larger than the measured values. For JETSET, the significance of a discrepancy is considerably larger than for HERWIG, which agrees within errors with our measurement, apart from the data point at the highest x_E. Generally, the measured values suggest a steeper fall with x_E than the models predict. However, this observation relies mainly on one measured point. A similar tendency towards a softer fragmentation than predicted by the models may also be observed in the neutral K^* results of [7], and similarly in the spectra of strange baryons in [9]. The $K^{*\pm}$ multiplicity per event is predicted by the HERWIG Monte Carlo to be 0.83. This value is in broad agreement with our measurement. The corresponding prediction of the JETSET Monte Carlo is 1.1, which is significantly larger than our measurement.

In JETSET, the probability that a strange meson carries spin 1 is controlled by a parameter often denoted[3] $\left(\frac{V}{P+V}\right)_s$ which has a default value of 0.6. This parameter was adjusted to describe the measured $K^{*\pm}$ rate, resulting in a value of 0.36 ± 0.05. The other model parameters were kept fixed. With this tuned parameter value, the predicted K^0 rate changes by $\simeq 2$ % and is still consistent with the value published previously [4]. A curve showing the JETSET prediction with the adjusted parameter setting is also shown in figure 3 where it is seen that agreement with the measurement is improved. Our adjusted value is consistent with a range of $\left(\frac{V}{P+V}\right)_s$ values of 0.4–0.5 found by [7] to describe the inclusive rates from LEP experiments published so far. The two results cannot be strictly compared, however, because they were obtained using different values of the parameter $\frac{s}{u}$, which describes the production probability of strange quarks from the sea.

[2] In HERWIG 5.0, the parameter values as determined by OPAL are the default values.

[3] In the JETSET code it is named PARJ(12).

Summary

We have measured the cross section for charged K^* production in e^+e^- collisions at centre–of–mass energies around the Z^0 pole. A multiplicity of $0.72 \pm 0.02 \pm 0.08$ $K^{*\pm}$ was found, which is lower than the JETSET prediction, but consistent with the HERWIG prediction. The JETSET model seems to require a lower value than the default one for the parameter which controls the production probability of strange vector mesons. Furthermore, the measurement shows some indications of a fragmentation function softer than predicted by the models. A similar effect has also been observed for neutral strange vector mesons [7]. The $K^{*\pm}$ rate measured at the Z^0 energy by [5] is larger than our value.

Acknowledgements

It is a pleasure to thank the SL Division for the efficient operation of the LEP accelerator, the precise information on the absolute energy, and their continuing close cooperation with our experimental group. In addition to the support staff at our own institutions we are pleased to acknowledge the
Department of Energy, USA,
National Science Foundation, USA,
Science and Engineering Research Council, UK,
Natural Sciences and Engineering Research Council, Canada,
Israeli Ministry of Science,
Minerva Gesellschaft,
Japanese Ministry of Education, Science and Culture (the Monbusho) and a grant under the Monbusho International Science Research Program,
American Israeli Bi-national Science Foundation,
Direction des Sciences de la Matière du Commissariat à l'Energie Atomique, France,
Bundesministerium für Forschung und Technologie, FRG,
National Research Council of Canada, Canada,
A.P. Sloan Foundation and Junta Nacional de Investigação Científica e Tecnológica, Portugal.

References

[1] B. Andersson et al., Phys. Rep. 97 (1983) 31.

[2] G.C. Fox and S. Wolfram, Nucl. Phys. B 168 (1980) 285;
S. Wolfram, Proc. of the XXVth Rencontre de Moriond, Les Arcs (France), March 1990, 549.

[3] L3 Collab., B. Adeva et al., Phys. Lett. B 259 (1991) 199.

[4] OPAL Collab., G. Alexander et al., Phys. Lett. B 264 (1991) 467.

[5] DELPHI Collab., P. Abreu et al., Phys. Lett. B 275 (1992) 231.

[6] ALEPH Collaboration, D. Buskulie et al., CERN PPE/92-74, submitted to Phys. Lett. B.;
L3 Collaboration, O. Adriani et al., Phys. Lett. B 286 (1992) 403.

[7] OPAL Collaboration, P. D. Acton et al., CERN PPE/92-116, to be published in Z. Phys. C.

[8] DELPHI Collaboration, P. Abreu et al., CERN PPE/92-183, submitted to Phys. Lett. B.

[9] OPAL Collaboration, P. D. Acton et al., Phys. Lett. B 291 (1992) 503.

[10] OPAL Collaboration, M.Z. Akrawy et al., Nucl. Instrum. Methods A 305 (1991) 275.

[11] O. Biebel et al., CERN PPE/92-55, submitted to Nucl. Instrum. Methods A.

[12] Particle Data Group, M. Aguilar–Benitez et al., Phys. Rev. D 45, Part 2 (1992).

[13] J. Allison et al., Nucl. Instr. Meth. A 317 (1992) 47.

[14] T. Sjöstrand, Comput. Phys. Commun. 39 (1986) 347;
T. Sjöstrand and M. Bengtsson, Comp. Phys. Comm. 43 (1987) 367.

[15] G. Marchesini and B.R. Webber, Nucl. Phys. B310 (1988) 461;
G. Marchesini, B.R. Webber et al., Comp. Phys. Comm. 67 (1992) 465.

[16] OPAL Collaboration, M.Z. Akrawy et al., Z. Phys. C 47 (1990) 505.

p (GeV/c)	x_E	$\overline{x_E}$	χ^2/dof	number of $K^{*\pm}$	$\frac{1}{\beta\sigma_{had}}\frac{d\sigma}{dx_E}$
0.00 – 2.75	0.020 – 0.064	0.037	0.79	2018	8.2 ± 1.6
2.75 – 4.00	0.064 – 0.090	0.076	1.18	1120	3.3 ± 0.7
4.00 – 6.00	0.090 – 0.133	0.110	1.16	1346	2.3 ± 0.6
6.00 – 8.00	0.133 – 0.177	0.154	1.27	1008	1.7 ± 0.4
8.00 – 12.50	0.177 – 0.275	0.221	0.99	1113	0.89 ± 0.23
12.50 – 40.00	0.275 – 0.879	0.417	0.88	662	0.11 ± 0.03

Table 1: Number of $K^{*\pm}$ observed, differential cross section for $K^{*\pm}$ production and χ^2 of fit.

Figure Captions

Figure 1. Invariant mass of $K^0_S\pi^\pm$ combinations.

Figure 2. Fits to the $K^0_S\pi^\pm$ mass spectra in momentum intervals. Momentum values are in GeV/c.

Figure 3. Fragmentation function (differential cross section) for $K^{*\pm}$ production.

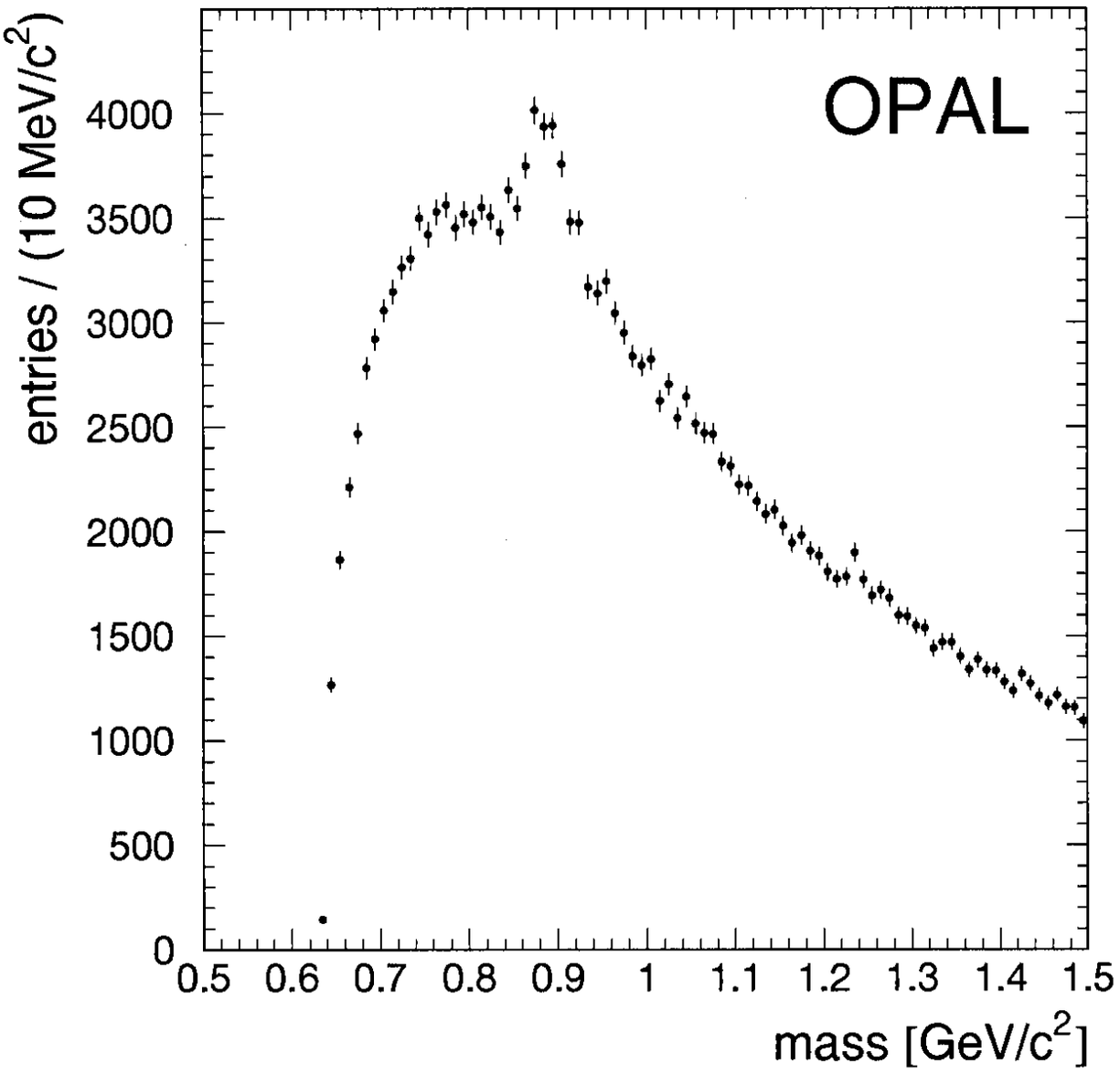
OPAL
entries / (10 MeV/c^2)
4000
3500
3000
2500
2000
1500
1000
500
0
0.5
0.6
0.7
0.8
0.9
1
1.1
1.2
1.3
1.4
1.5
mass [GeV/c^2]

Figure 1

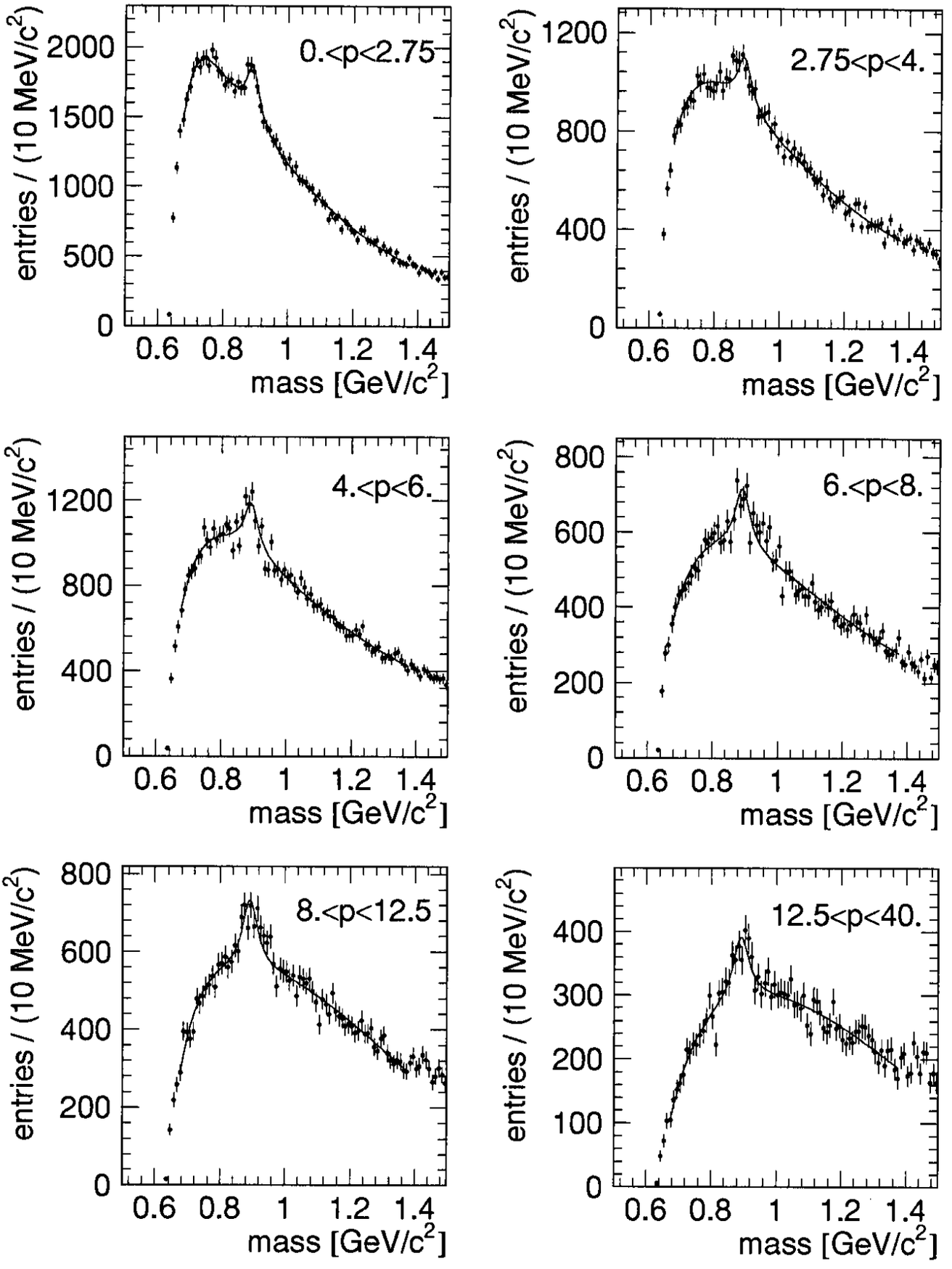
0.<p<2.75
2.75<p<4.
4.<p<6.
6.<p<8.
8.<p<12.5
12.5<p<40.
entries / (10 MeV/c²)
mass [GeV/c²]

Figure 2

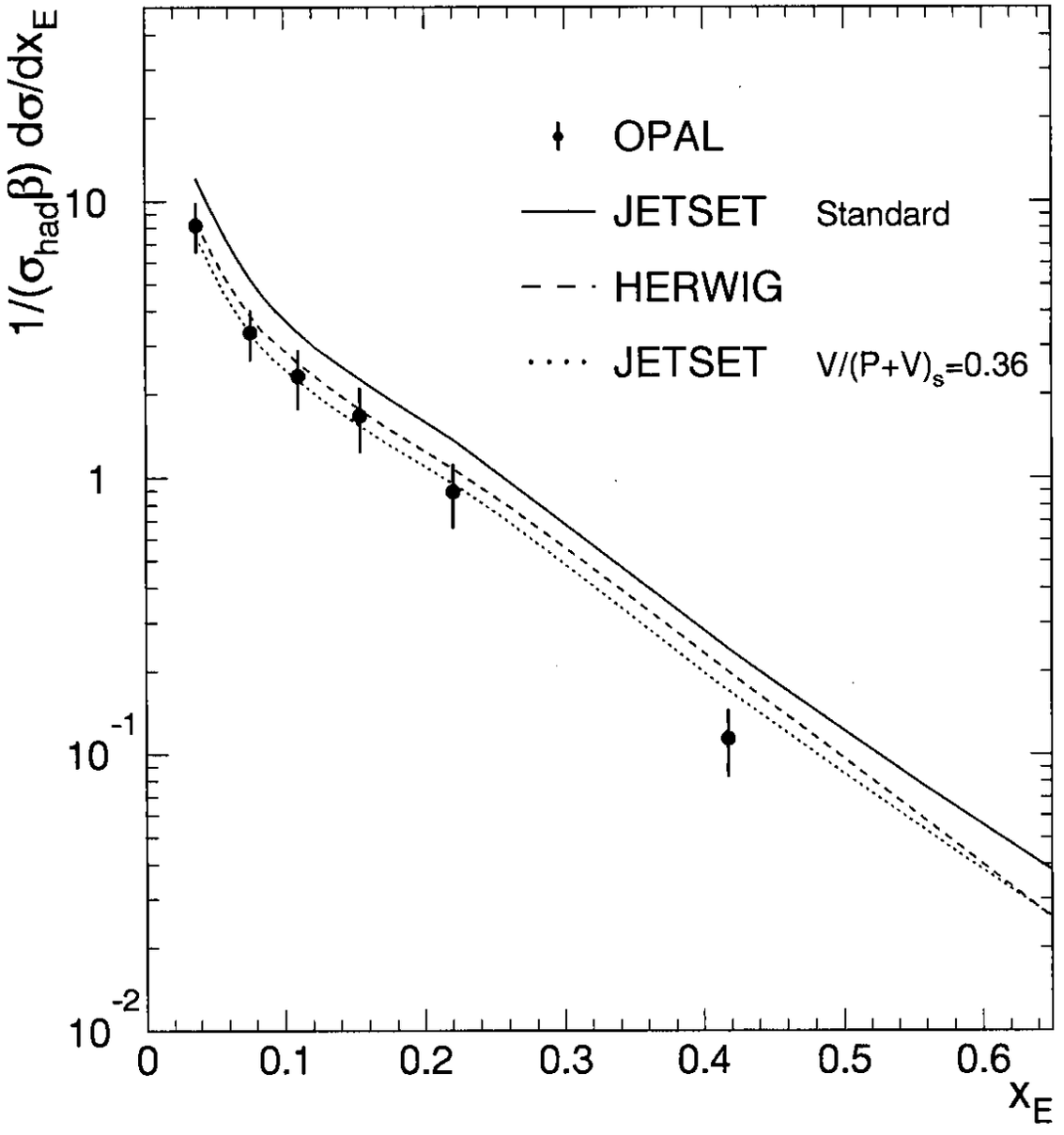
$1/(\sigma_{had}\beta)\ d\sigma/dx_E$
10
1
10^{-1}
10^{-2}
0
0.1
0.2
0.3
0.4
0.5
0.6
x_E
OPAL
JETSET Standard
HERWIG
JETSET $V/(P+V)_s$=0.36

Figure 3